Ribosomal Components Neighboring the Conserved 518–533 Loop of 16S rRNA in 30S Subunits†

Rebecca W. Alexander, Parimi Muralikrishna, and Barry S. Cooperman*

Department of Chemistry, University of Pennsylvania, Philadelphia, Pennsylvania 19104-6323

Received May 23, 1994; Revised Manuscript Received July 25, 1994®

ABSTRACT: We report the synthesis of a radioactive, photolabile oligodeoxyribonucleotide probe complementary to 16S rRNA nucleotides 518–526 and its exploitation in identifying 30S ribosomal subunit components neighboring its target site in 16S rRNA. Nucleotides 518–526 lie within an almost universally conserved single-stranded loop that has been linked to the decoding region of *Escherichia coli* ribosomes. On photolysis in the presence of activated 30S ribosomes, the probe site-specifically incorporates into proteins S3, S4, S7, and S12 (identified by SDS–PAGE, RP-HPLC, and immunological analysis); nucleotides C525, C526, and G527 adjacent to its target binding site; and the 3′-terminus of 16S rRNA. When the probe is photoincorporated into 30S subunits subjected to brief cold inactivation (SI subunits), S7 labeling is increased compared to activated subunit incorporation, while S3, S4, and S12 labeling is decreased, as is labeling to nucleotides C525, C526, and G527; labeling at the 16S rRNA 3′-terminus appears unchanged. Longer cold inactivation of the 30S subunits (LI subunits) leads to decreases in the labeling of all components. These results provide clear evidence that C526 lies within 24 Å (the distance between C526 and the photogenerated nitrene) of proteins S3, S4, S7, and S12 and the 3′-terminus of 16S rRNA. The identity of the tryptic digestion patterns of S7 labeled with the probe complementary to 16S rRNA nucleotides 518–526 and with a probe complementary to nucleotides 1397–1405 [Muralikrishna, P., & Cooperman, B. S. (1994) *Biochemistry 33,* 1392–1398] also provides evidence for proximity between C526 and G1405. Our results support the conclusion of Dontsova et al. [Dontsova, O., et al. (1992) *EMBO J. 11,* 3105–3116] in placing the 530 loop in close proximity to the decoding center of the 30S subunit but are apparently inconsistent with some protein–protein distances determined by neutron diffraction [Capel, M. S., et al. (1988) *J. Mol. Biol. 200,* 65–87]. This inconsistency suggests that a multistate model of subunit conformation may be required to account for the totality of results pertaining to the internal structure of the 30S subunit.

The region of *Escherichia coli* 16S ribosomal RNA including nucleotides 518–533 is a single-stranded loop that is almost universally conserved (Woese et al., 1975; Gutell et al., 1985). Immunoelectron microscopy places this 530 loop at the level of the neck on the cytoplasmic side of the 30S subunit (Oakes & Lake, 1990; Oakes et al., 1990; Lasater et al., 1990), at or near the binding sites for elongation factors Tu (Langer & Lake, 1986) and G (Girshovich et al., 1974). Both biochemical and genetic evidence clearly implicate the 530 loop in ribosomal function, at the level of both the accuracy control mechanism and the A-site binding of aminoacyl-tRNA. For example, the presence of A-site-bound tRNA protects nucleotides in the loop from kethoxal attack (Moazed & Noller, 1986), and binding of antibiotics of the neomycin class enhances chemical reactivity of C525 (Moazed & Noller, 1987). Futhermore, mutations at G530 prevent polysome formation, leading to cell death (Powers & Noller, 1990, 1991). The G530A mutation produces ribosomes defective in EF-Tu-dependent aminoacyl-tRNA binding (Powers & Noller, 1993), while the G530U mutation causes a significant decrease in mRNA-dependent fMet-Val dipeptide synthesis (Santer et al., 1993). In addition, mutations at G517 produce readthrough and frameshift errors (O'Connor et al., 1992), and the G to A mutation at the equivalent base in yeast (G633) suppresses the mitochondrial ochre mutation (Shen & Fox, 1989). Finally, ribosomes containing the 523 A to C mutation are resistant to the error-inducing antibiotic streptomycin (Melançon et al., 1988).

The 530 loop region has been shown to be accessible to complementary oligodeoxyribonucleotide probes, which competitively inhibit poly(U) binding to the 30S subunit (Hill et al., 1990). Implementing techniques developed in this laboratory (Muralikrishna & Cooperman, 1991, 1994), we use the photolabile oligodeoxyribonucleotide probe *O*-(6-((*p*-azidobenzoyl)amino)hexyl)-pGGCTGCTGGA* (ABAH526–518A*,[1] where the asterisk indicates the presence of radioactivity), complementary to 16S rRNA nucleotides 518–526, to identify the 30S ribosomal components proximal to the conserved 530 loop. We find clear evidence that the 530 loop is at or near the decoding center of the 30S subunit, in agreement with related results of Dontsova et al. (1992), present evidence for conformational change within the 30S subunit between activated and inactivated subunits, and consider apparent inconsistencies between our results and the model of protein placement within the 30S subunit put forward by Capel et al. (1988).

† This work was supported by NSF Grant MCB-9118072 and by NSF Predoctoral Fellowship RCD91-54685 to R.W.A.

* Author to whom inquiries should be addressed.

® Abstract published in *Advance ACS Abstracts,* September 1, 1994.

[1] Abbreviations: ABAH, *O*-(6-((*p*-azidobenzoyl)amino)hexyl)-; ActA and ActB subunits, 30S subunits that have been heat activated; AMV-RT, avian myeloblastosis virus reverse transcriptase; DMT, dimethoxytrityl; HSAB, *N*-hydroxysuccinimidyl 4-azidobenzoate; LI subunits, 30S subunits subjected to a long period of cold inactivation; PAGE, polyacrylamide gel electrophoresis; RP-HPLC, reverse-phase high-performance liquid chromatography; SI subunits, 30S subunits subjected to a short period of cold inactivation; TP30, total protein from 30S subunits.

0006-2960/94/0433-12109$04.50/0

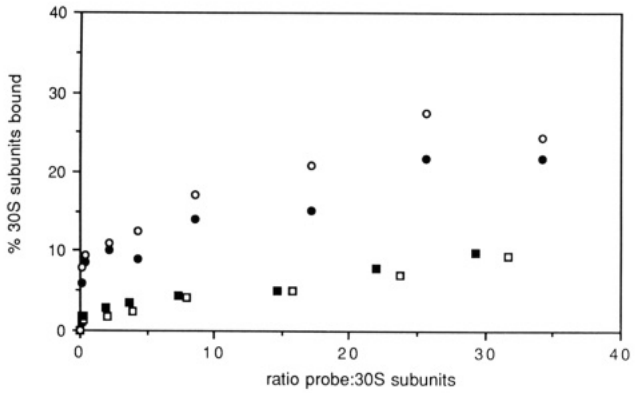

FIGURE 1: Binding of p*526–518 to 30S subunits. 30S subunits (15 pmol) were incubated with varying amounts of p*526–518 (400–500 cpm/pmol) as described in Methods. The initial volume of TMK0.3 buffer was 25 μL. Reaction mixtures were diluted with 0.5 mL of cold TKM0.3 containing 10 mM $MgCl_2$ and filtered through HAWP 0.45-μm nitrocellulose filters (Millipore), followed by three 1-mL washes of the filter with binding buffer. The amount of filter-bound oligonucleotide was determined by liquid scintillation counting of the dried filters. ActA (●), ActB (○), SI (■), LI (□).

EXPERIMENTAL PROCEDURES

Materials

Buffers. TKM0.3: 40 mM Tris-HCl (pH 7.4), 60 mM KCl, and 0.3 mM $MgCl_2$; TBE: 89 mM Tris–borate (pH 8.3) and 8 mM EDTA. TND: 20 mM Tris-HCl (pH 7.9), 100 mM NaCl, and 1 mM dithiothreitol.

Except as indicated, all materials, including inactivated and activated 30S subunits, were obtained as described previously (Muralikrishna & Cooperman, 1991, 1994). Dimethyl sulfate (Aldrich), trypsin (Sigma), $tRNA^{Phe}$ (Boehringer Mannheim Biochemicals), and [^{3}H]Phe (Amersham) were obtained from the vendors indicated.

Synthesis and Purification of Oligodeoxyribonucleotides. All of the oligonucleotides used in this work were made and purified by procedures essentially identical to those employed earlier (Muralikrishna & Cooperman, 1991, 1994). They are as follows cDNA 526–518, having the sequence 5′-GGCTGCTGG-3′; MM-cDNA 526–518, the corresponding mismatched oligonucleotide having the sequence 5′-GGCGTCTGG-3′; p*526–518, the 5′-^{32}P-phosphorylated derivative of cDNA 526–518; ABAH526-518, the 5′-*O*-(6-((*p*-azidobenzoyl)amino)hexyl) derivative of cDNA; ABAH526–518A*, the ^{32}P-labeled 3′-dideoxyadenylyl derivative of ABAH526–518; cDNA 811–03 (23S rRNA), having the sequence 5′-AACCAGCTA-3′.

An HPLC-purified sample of S7 that had been photoaffinity labeled with ABAH1405–1397A* was prepared as described in Muralikrishna and Cooperman (1994).

Methods

Except as indicated, all methods were performed as described previously (Muralikrishna & Cooperman, 1991, 1994).

Oligonucleotide Binding and Photoincorporation Experiments. These experiments were carried out with 30S subunits prepared in four different manners and denoted activated A (ActA), activated B (ActB), short-inactivated (SI), and long-inactivated (LI).

ActA and ActB 30S subunits were each activated by heating at 38 °C for 20 min in the presence of 10 mM Mg^{2+} (Zamir et al., 1971). Each type was then briefly incubated with probe cDNA in TKM0.3 at 0 °C, heated at 37 °C for 5 min, and left on ice for 10–15 min, after which time the $MgCl_2$ concentration was raised to 10 mM. ActA subunits were then heated to 37 °C for 5 min, and incubation on ice was continued for 2–3 h prior to binding measurements or photoincorporation experiments (3000-Å lamps, 4 min, 4 °C). ActB subunits were treated similarly, except that the final 5-min heating step was omitted.

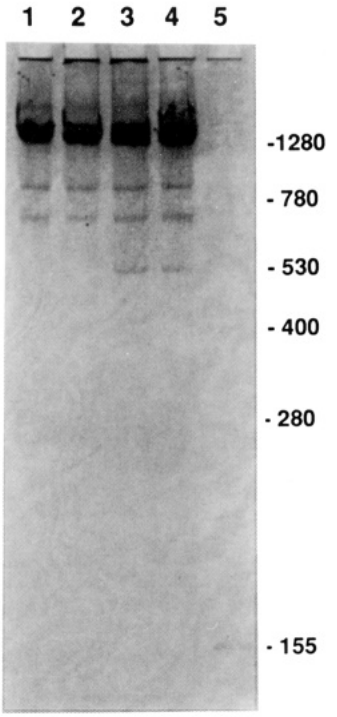

FIGURE 2: Urea–PAGE analysis of RNase H digestions. Complexes of ActB subunits (75 pmol) and either cDNA 526–518 or ABAH526–518 (150 pmol) in 50 mM Tris (pH 7.6), 100 mM KCl, and 10 mM $MgCl_2$ (25 μL) were digested for 12–16 h at 0 °C with RNase H (10 units). The phenol:chloroform extracted RNA was analyzed by electrophoresis on a 5% polyacrylamide/0.25% bis(acrylamide)/7 M urea gel made up in TBE buffer. RNA was detected with methylene blue. Lane 1, 16S rRNA from undigested subunits; lane 2, RNase H with no added cDNA; lane 3, RNase H with cDNA 526–518; lane 4, RNase H with ABAH526–518; lane 5, RNA size markers.

Neither SI nor LI subunits were heat activated. SI subunits were incubated with probe cDNA in TKM0.3 at 0 °C for 15 min, after which the $MgCl_2$ concentration was raised to 10 mM, and incubation on ice was continued for 2–3 h prior to binding measurements or photoincorporation experiments. For LI subunits, incubation with probe cDNA in TKM0.3 at 0 °C was continued for 16–20 h prior to raising $MgCl_2$ concentration to 10 mM, incubating for 2–3 h on ice, and performing binding measurements or photoincorporation experiments.

The *N*-acetyl-Phe-$tRNA^{Phe}$ binding activities of the 30S preparations fell in the order untreated 30S (1.00) > ActA (0.44 ± 0.13) > ActB, SI > LI (<0.05). The relative activities found for ActB and SI preparations were quite variable, ranging from 0.09 to 0.30. Untreated 30S subunits bound 0.50 ± 0.09 *N*-acetyl-Phe-$tRNA^{Phe}$ per subunit.

Quantification of Protein Labeling. Labeled 30S proteins were prepared for RP-HPLC as described previously (Muralikrishna & Cooperman, 1994). Net radioactivity eluting in protein peaks was calculated by subtracting baseline ^{32}P counts per minute from observed ^{32}P counts per minute. The same number of fractions were summed for each determination of the same protein peak, although this number varied for different protein peaks. Reported percent incorporation corresponds to picomoles of ^{32}P-labeled protein per 100 pmol of total protein as determined by comparison of the sum of

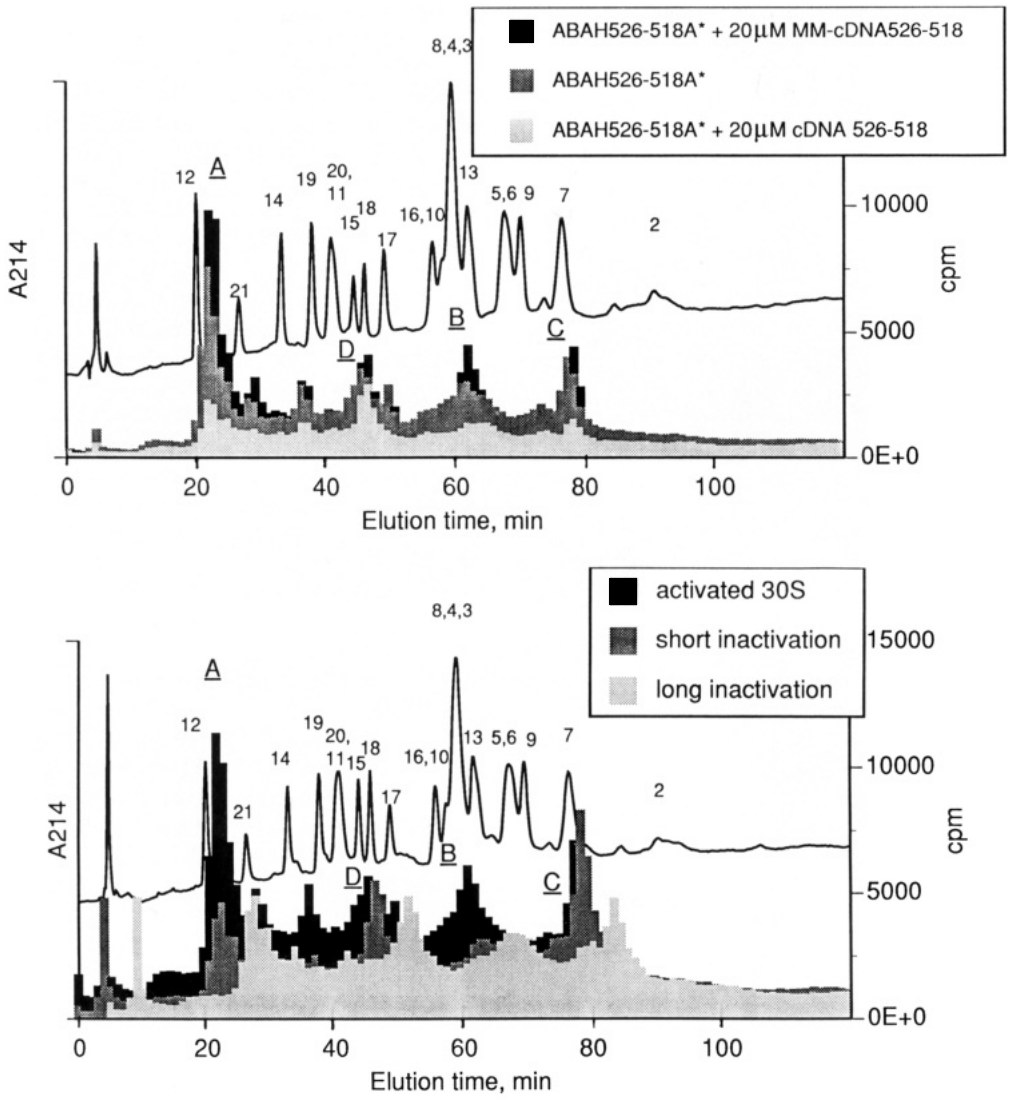

FIGURE 3: RP-HPLC analyses of TP30 from 30S subunits photolyzed with ABAH526–518A*. Upper panel: Effect of added oligoDNAs on labeling of ActB TP30. The initial reaction mixture (total volume, 75 μL) contained ActB subunits (150 pmol) and ABAH526–518A* (10 pmol) in the absence or presence (1500 pmol) of added oligoDNAs. The low stoichiometry of ABAH526–518A* utilized maximizes specific photoincorporation. For each analysis, proteins were extracted from photolyzed subunits with 67% acetic acid, precipitated with acetone, redissolved in 200 μL of 0.1% trifluoroacetic acid, applied to a SynChropak RP-P column, and eluted at a flow rate of 0.7 mL/min with a 120-min 15–45% convex acetonitrile gradient containing 0.1% trifluoroacetic acid (Kerlavage et al., 1983). Lower panel: Comparison of labeled TP30 from ActB, SI, and LI subunits. Protocols as described for upper panel. The cpm profile for LI subunits is offset +5 min for clarity.

the A_{214} peak areas of 30S proteins with a standard of bovine serum albumin (Buck et al., 1989).

Analysis of Tryptic Peptides. RP-HPLC-purified ribosomal protein S7 photoaffinity labeled from activated 30S subunits with ABAH526–518A* or ABAH1405–1397A* was dissolved in 10 mM triethanolamine-HCl (pH 8.0, 0.3 mg/mL) and digested with trypsin. Five milligrams of each labeled S7 sample was quenched in 0.1% SDS/ 10 mM 2-mercaptoethanol, heated to 65 °C for 10 min, and electrophoresed on a 20% polyacrylamide/SDS gel according to Muralikrishna and Cooperman (1991).

Dimethyl Sulfate Modification. The procedure of Moazed, et al. (1986a) was altered to allow hybridization of the oligoDNA probe. In a total reaction volume of 300 μL, 30S subunits (80 pmol) in 30 mM potassium cacodylate (pH 7.2) and 0.3 M KCl were incubated for 5 min at 37 °C and 10 min on ice either in the absence of oligoDNA or in the presence of a 20-fold excess (1.6 nmol) of either cDNA 526–518, ABAH526–518, or MM-cDNA 526–518. The reaction mixtures were brought to 20 mM in magnesium acetate and incubated for an additional 15 min on ice. One microliter of DMS was added to each reaction mixture, and incubation was continued for 90 min on ice before the addition of 75 μL of stop buffer (1.0 M Tris–acetate, pH 8.0, 1.0 M 2-mercaptoethanol, 1.5 M sodium acetate, pH 5.2, and 0.1 mM EDTA). The subunits were precipitated with 2.5 vol of EtOH, and modified rRNA was recovered on a 5–20% sucrose/urea–SDS gradient. DMS-modified nucleotides were identified by reverse transcriptase-catalyzed primer extension.

tRNA Binding Assay. Poly(U)-directed Phe-tRNA binding to 30S subunits was carried out according to Zamir et al. (1971), as follows: 30S subunits (15 pmol), prepared as described above but with cDNA probe omitted, were incubated with 30 pmol of *N*-acetyl-[^{3}H]Phe-tRNA^{Phe} and 5 μg of poly(U) in 50 mM Tris-HCl (pH 7.5), 30 mM magnesium acetate, and 150 mM NH_4Cl (total volume, 50 μL). After incubation for 1 h on ice, the reaction mixtures were quenched with 1.5 mL of cold wash buffer (10 mM Tris-HCl (pH 7.5), 10 mM magnesium acetate, and 50 mM NH_4Cl), passed through 0.45-μm nitrocellulose filters (Millipore HAWP), and washed with four 2-mL portions of cold wash buffer. Filters were dried and counted in Ecolite(+) liquid scintillation cocktail.

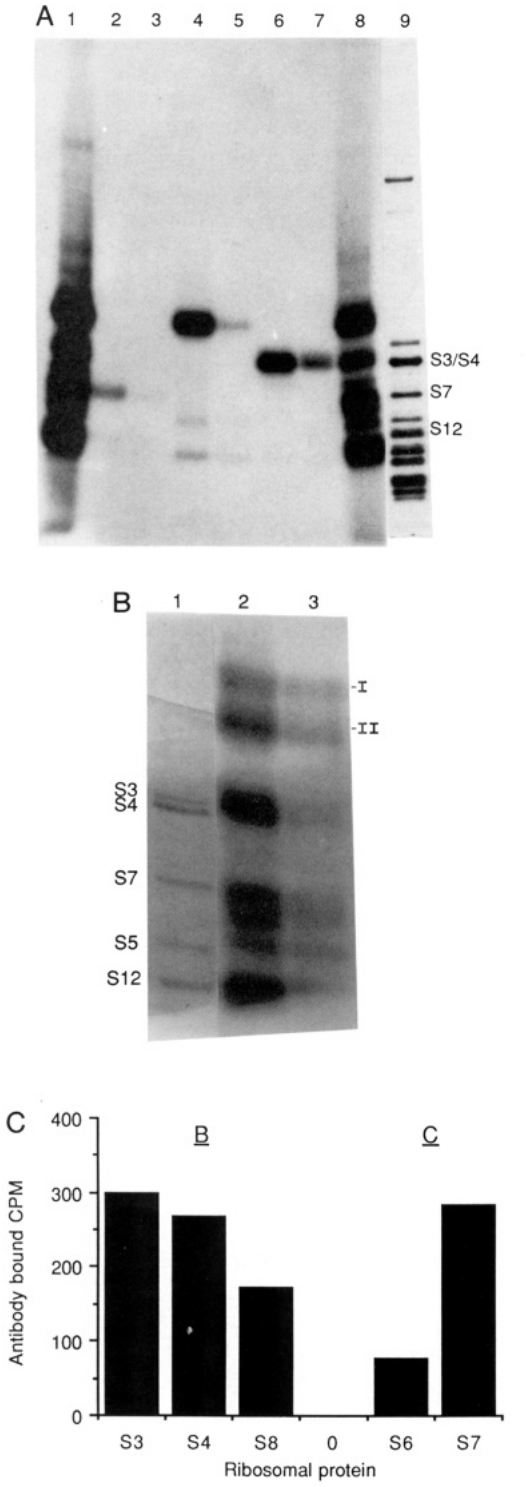

FIGURE 4: SDS–PAGE and immunological identification of labeled proteins from ActB subunits. Panel A: Autoradiogram of an SDS–PAGE analysis of ABAH526–518A*-labeled proteins separated by HPLC. Lanes 1 and 8, TP30 from ActB subunits photolyzed with ABAH526–518A*. Lanes 2, 4, and 6, peaks A, B, and C, respectively (see Figure 3A), for the sample labeled in the absence of added cDNA 526–518; lanes 3, 5, and 7, peaks A, B and C, respectively, for the sample labeled in the presence of added cDNA 526–518; lane 9, TP30 stained with Coomassie Blue. The gel was prepared with 15% acrylamide/0.08% bis(acrylamide) in 0.75 M Tris-HCl (pH 8.8)/0.1% SDS. Panel B: Autoradiogram of an SDS–PAGE analysis of ABAH526–518A*-labeled TP30 from ActB subunits photolyzed in the absence (lane 2) or presence (lane 3, 10-fold excess over subunits) of cDNA 526–518; lane 1, Coomassie Blue-stained 30S proteins. The gel was prepared with 18% acrylamide/0.1% bis-(acrylamide) in 0.75 M Tris-HCl (pH 8.8)/0.1% SDS. Bands I and II correspond to labeled S3 and S4, respectively. Panel C: Agarose antibody affinity chromatography analysis of RP-HPLC peaks B and C.

RESULTS

Noncovalent Binding of Deoxyoligonucleotides to 30S Subunits. The noncovalent binding of cDNA p*526–518 to 30S subunits was determined using a Millipore assay (Figure 1). ActA and ActB subunits give similar results: approximately 20% of the activated subunits bind the oligonucleotide, nearly reaching this plateau level at a probe:30S subunit molar ratio of 8:1. SI and LI subunits bind less p*526–518 probe, each reaching approximately 10% of 30S subunits bound at a probe:subunit ratio of 30:1.

Evidence that at least some of the binding of p*526–518 to ActB subunits occurs to its complementary region in 16S rRNA is provided by the 520-nt RNA fragment generated upon RNaseH treatment of 16S rRNA (Figure 2) in the presence of either cDNA 526–518 (lane 3) or cDNA ABAH526–518 (lane 4). The fragment is not formed in the absence of either oligonucleotide or RNaseH (lanes 1 and 2). Similar results were obtained with SI subunits (data not shown).

Proteins S12, S3, S4, and S7 Are Specifically Labeled on Photolysis of Activated 30S:ABAH526–518A Complexes.* Proteins extracted from ActB subunits photolabeled by ABAH526–518A* were analyzed by RP-HPLC (Figure 3A). Four major labeled peaks are observed, A–D. Photoincorporation into three of these peaks, A–C, is markedly decreased in the presence of cDNA 526–518 but not in the presence of MM-cDNA 526–518, demonstrating that these peaks are labeled site-specifically. Peaks A and C co-elute with the well-resolved proteins S12 and S7, respectively. Peak B, however, elutes as a broad peak in a crowded region of the chromatogram that includes proteins S3, S4, S8, and S13. Photoincorporation into peak D, comigrating with protein S18, is not appreciably decreased in the presence of cDNA 526–518, indicating that such labeling is not site-specific. Protein S18 is unusually nucleophilic and has been shown to be non-site-specifically labeled in several other affinity labeling studies (Cooperman, 1980).

Further information regarding the identity of specifically labeled proteins in peaks A–C was provided by SDS–PAGE analysis coupled with autoradiography and by immunological analysis. We have shown previously (Muralikrishna & Cooperman, 1991, 1994) that ribosomal protein labeled with an oligoDNA migrates in SDS–PAGE with an apparent molecular mass corresponding approximately to the sum of the protein and oligoDNA masses. In what follows we distinguish between actual molecular mass, calculated from a knowledge of ribosomal protein primary structure (Giri et al., 1984), and apparent molecular mass, calculated by comparison of observed band migration with a best-fit line through a plot of band migration vs the logarithm of actual molecular masses for TP30.

The single radioactive band migrating with an apparent molecular mass of 16.7 kDa in lane 2 of Figure 4A is clearly consistent with peak A representing labeled S12. S12 has an apparent molecular mass of 13.5 kDa and an actual molecular mass of 13.6 kDa. Similarly, peak C yields one highly radioactive band having an apparent molecular mass of 21.2 kDa (lane 6) and can be identified as labeled S7. S7 has an apparent molecular mass of 19.0 kDa and an actual molecular mass of 19.7 kDa. Peak B also yields one highly radioactive band migrating at 26.7 kDa (lane 4), but S3 and S4 are not sufficiently well resolved to determine whether the radioactive band corresponds to labeled S3 or S4, or both. S3 has an apparent molecular mass of 22.2 kDa and an actual molecular mass of 25.8 kDa, while S4 has an apparent molecular mass of 21.3 kDa and an actual molecular mass of 23.1 kDa. The

Table 1: Relative Protein Photoincorporation of ABAH526–518A* into Protein Peaks Derived from Labeled 30S Subunits[a]

	protein	30S subunit ActA	ActB	SI	LI
series 1: relative to incorporation into S12	S12	(1.00)	(1.00)[b]	(1.00)	(1.00)
	S3/S4	0.39 ± 0.01	0.55 ± 0.10	0.46 ± 0.08	0.52 ± 0.06
	S7	0.47 ± 0.08	0.43 ± 0.13	0.92 ± 0.19	0.45 ± 0.08
no. of detns.		2	17	7	3
series 2: relative to incorporation into ActB subunits	S12	1.00 ± 0.01	(1.00)[b]	0.66 ± 0.06	0.62 ± 0.10
	S3/4	0.74 ± 0.09	(1.00)	0.64 ± 0.14	0.61 ± 0.08
	S7	1.33 ± 0.06	(1.00)	1.98 ± 0.69	0.60 ± 0.07
no. of detns.		2		7	3

[a] Estimated from RP-HPLC data, as in Figure 3. Labeling of proteins S12, S3/S4, and S7 was estimated from the radioactivity in peaks A, B, and C, respectively. Average deviations are indicated. [b] Corresponds to a labeling stoichiometry of 0.10 ± 0.02%.

much greater labeling seen in lanes 2, 4, and 6, derived from samples labeled in the absence of cDNA 526–518, than in lanes 3, 5, and 7, derived from samples labeled in the presence of cDNA 526–518, respectively, provides another demonstration of the site-specific character of S12, S3/S4, and S7 labeling.

Clarification of the identity of peak B is provided by the autoradiogram of an SDS–PAGE analysis of TP30 carried out to achieve clear resolution of S3 and S4 (Figure 4B). Bands I and II in lanes 2 and 3 correspond to labeled S3 and labeled S4, respectively. The results clearly demonstrate that both S3 and S4 are site-specifically labeled, with S4 labeling proceeding in greater yield. The presence of labeled S3 and S4 within peak B is also supported by antibody affinity chromatography analysis; S8, which elutes with S3 and S4, may be a nonspecifically labeled component of peak B (Figure 4C). This technique was also used to confirm the identity of peak C as labeled S7, using S6, which elutes near S7, as a negative control. Antibody to S12 was not available for testing of peak A.

Proteins extracted from ActA subunits photolabeled by ABAH526–518A* give a pattern of labeling on RP-HPLC analysis and SDS–PAGE analysis similar to that shown for ActB subunits (Table 1, series 1), although labeling of S3/S4 is somewhat decreased and labeling of S7 is somewhat increased (Table 1, series 2). The effects of added cDNA 526–518 in decreasing the labeling of peaks A–C and in not decreasing labeling of peak D are also quite similar to what is seen for ActB subunits.

Protein Labeling on Photolysis of Inactivated 30S: ABAH526–518A Complexes.* Experiments paralleling those described above were performed on complexes between SI or LI subunits and ABAH526–518A*. In a comparison of SI with ActB subunits, incorporation into peaks A and B is substantially reduced and incorporation into peak C is substantially increased, whereas with LI subunits incorporation into peaks A–C is substantially reduced (Figure 3B; Table 1). As with proteins from activated subunits, incorporation into peaks A, B, and C from both SI and LI subunits is reduced when cDNA 526–518 is present in the photolysis mixture, while incorporation into peak D is not reduced. The correspondence of peaks A, B, and C to proteins S12, S3/S4, and S7, respectively, was confirmed using one-dimensional SDS–PAGE analysis, as above.

Proteins S3/S4, S7, and S12 Are Labeled in ActB 30S Subunits with Similar K_ds. The decrease in radioactivity in HPLC peaks A, B, and C as a function of added cDNA 526–518 is presented in Figure 5. For each peak, these data can be fitted to eq 1, in which F is the fraction of radioactivity

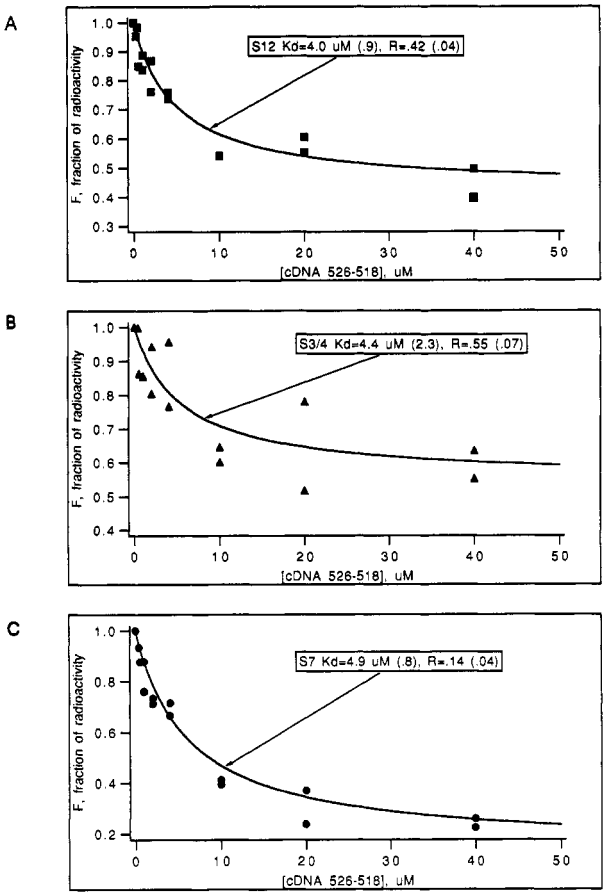

FIGURE 5: Photoincorporation of ABAH526–518A* into RP-HPLC peaks A, B, and C as a function of cDNA 526–518 concentration. Photoincorporation of ABAH526–518A* into ActB 30S subunits in the presence of variable amounts of cDNA 526–518 and subsequent RP-HPLC analysis of labeled TP30 were carried out as described (see Figure 3 caption). The curve-fitting program IGOR (Wavemetrics, P.O. Box 2088, Lake Oswego, OR 97035) was used to determine K_d and R values according to eq 1; for peaks A (labeled S12), B (labeled S3 and S4), and C (labeled S7), respectively, these values are 4.0 ± 0.9 μM, 0.42 ± .04; 4.4 ± 2.3 μM, 0.55 ± .07; and 4.9 ± 0.8 μM, 0.14 ± .04 .

$$F = [K_d/(K_d + C)][1 - R] + R \quad (1)$$

remaining in the peak at a given concentration, C, of added cDNA 526–518, K_d is the dissociation constant for the binding of cDNA 526–518 that competes with the binding of ABAH526–518A* to the site leading to photoincorporation, and R represents the residual fraction of radioactivity remaining in the peak at $C \gg K_d$, including radioactivity due

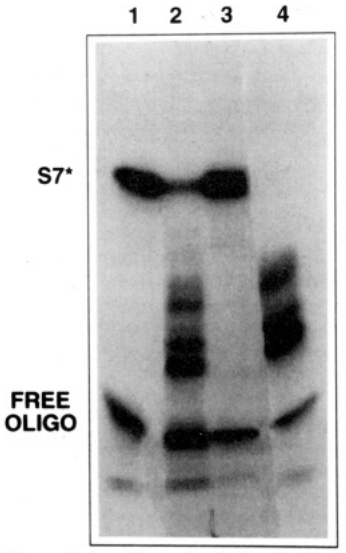

FIGURE 6: PAGE analysis of tryptic digestion products of labeled protein S7. Autoradiogram of SDS–PAGE analysis of ABAH526–518A*-labeled S7 before (lane 1) and after (lane 2) trypsin digestion and of ABAH1405–1397A*-labeled S7 before (lane 3) and after (lane 4) trypsin digestion. In both cases, trypsin digestion was carried out at an S7:trypsin ratio of 30:1 at 37 °C for 30 min.

to nonspecific labeling of contaminating proteins.

The K_d values for all three peaks, ranging from 4.0 to 4.9 μM, are essentially indistinguishable from one another, consistent with a single oligo binding site responsible for protein labeling observed in the three peaks.[2]

Tryptic Digestion of Protein S7 Photolabeled with ABAH526–518A and with ABAH1405–1397A**. Tryptic digestion of labeled S7 produces a fragment pattern, as observed by autoradiography of an SDS–PAGE analysis, that is identical whether the labeled S7 was purified from activated 30S subunits labeled by the cDNA probe ABAH526–518A* or the probe ABAH1405–1397A* (Figure 6). These tryptic digests indicate that the two probes insert into the same or similar sites. Such sites have not as yet been identified at the amino acid level.

Photoincorporation of ABAH526–518A into 16S rRNA.* Photolysis of ActA or ActB complexes with ABAH526–518A* gives essentially identical incorporation results at all levels of analysis. Thus, in presenting the 16S rRNA results, we drop the distinction between ActA and ActB subunits.

Photoincorporation of ABAH526–518A* into 16S rRNA of activated subunits is light-dependent, almost completely abolished on addition of cDNA 526–518, and unaffected by the addition of MM-cDNA 526–518. For the experiment depicted in Figure 7 the levels of incorporation, expressed as percentage of 30S subunits, are as follows: full experiment, 0.31; minus irradiation, 0.001; plus added cDNA 526–518, 0.03; plus added MM-cDNA 526–518, 0.35.

Photolysis of a complex formed between SI subunits and ABAH526–518A* gives similar results except that photoincorporation is about 50% of that obtained with activated subunits. Addition of cDNA 526–518 nearly eliminates photoincorporation, while addition of MM-cDNA 526–518 has a negligible effect (data not shown).

Partial Localization of ABAH526–518A Photoincorporation Sites in 16S rRNA.* Partial localization of oligoDNA photoincorporation into the rRNA fraction of labeled 30S subunits was carried out by PAGE and autoradiographic

[2] In an earlier account of some of this work (Cooperman et al., 1993), an editorial error resulted in these dissociation constants being reported as 2–3 nM.

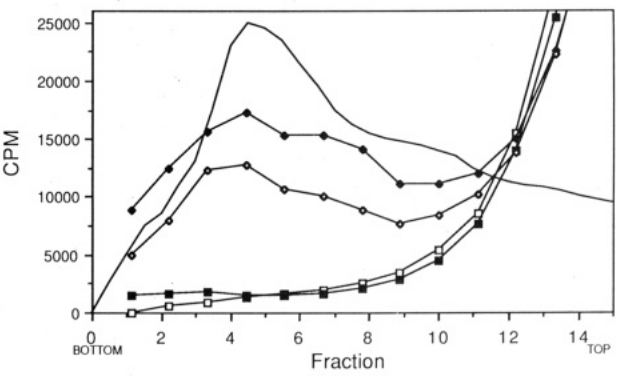

FIGURE 7: Photoincorporation of ABAH526–518A* into 16S rRNA: activated subunits (150 pmol) that had been incubated with ABAH526–518A* (50 pmol): (□) without photolysis, (◆) with photolysis, (■) with photolysis in the presence of cDNA 526–518 (1500 pmol), and (◇) with photolysis in the presence of MM-cDNA 526-518 (1500 pmol). After photolysis, subunits were EtOH-precipitated and dissolved in 200 μL of 25 mM sodium acetate (pH 5.2) containing 7 M urea and 1% SDS. After being heated to 55 °C for 10 min, samples were subjected to ultracentrifugation through a urea–SDS sucrose gradient. The solid line without symbols is a trace of absorbance at 260 nm, with the peak corresponding to the elution position of 16S rRNA.

analysis of the products of RNase H treatment (Figure 8). The apparent sizes of labeled fragments (as estimated from a semilog plot of the number of nucleotides vs migration distance for a set of RNA size markers, lane 1) are typically larger (10–20 nt) than would be expected for the corresponding unlabeled fragments generated with complete RNase H digestion. This is due to the size of both the photoincorporated probe itself (10 nts) and the "frayed" ends that sometimes result from incomplete RNase H digestion.

RNase H digestion of ABAH526–518A*-labeled 16S rRNA derived from activated 30S subunits reveals the presence of a ^{32}P-labeled ~1000-nt fragment (Figure 8A, lane 3), indicating both that the specific heteroduplex between photolyzed, covalently incorporated ABAH526–518A* and 16S rRNA is reformed under the conditions used for RNase H digestion, providing a site for RNase H cleavage, and that photoincorporation into 16S rRNA takes place between nucleotides 518–526 and 1542. As expected, the intensity of this band is unaffected by the addition of cDNA 268–259 prior to RNase H treatment (Figure 8A, lane 4). Addition of cDNA 565–556 (Figure 8A, lane 5) produces an intense band approximately 45 nt long, while addition of cDNA 795–787 (Figure 8A, lane 6) yields an intense band approximately 280 nt long. Also visible in lane 6 is a less intense band approximately 750 nt long. These results permit the conclusion that photoincorporation of ABAH526–518A* into activated 30S subunits occurs primarily between nucleotides 518–526 and 556–565 with a lesser amount of photoincorporation between nucleotides 787–795 and 1542. The addition of cDNA probes progressively nearer the 3′-terminus of 16S rRNA produces progressively smaller labeled fragments (Figure 8A, lanes 7–11; Figure 8B, lanes 2–4). The smallest labeled fragment produced, a 14-mer that includes the 10-nt probe, locates the minor labeling site between nucleotides 1539 and 1542 at the 3′-terminus.

Labeled fragments of activated 30S subunit-derived 16S rRNA, produced by RNase H digestion in the presence of cDNA 565–556 (45 nt) and cDNA 1339–1330 (220 nt), provide convenient monitors of photoincorporation into the two sites described above. Photoincorporation into both of these locations is site-specific, since in each case it is strongly decreased when photolysis is carried out in the presence of cDNA 526–518 (Figure 8C, compare lanes 1 and 2 and lanes

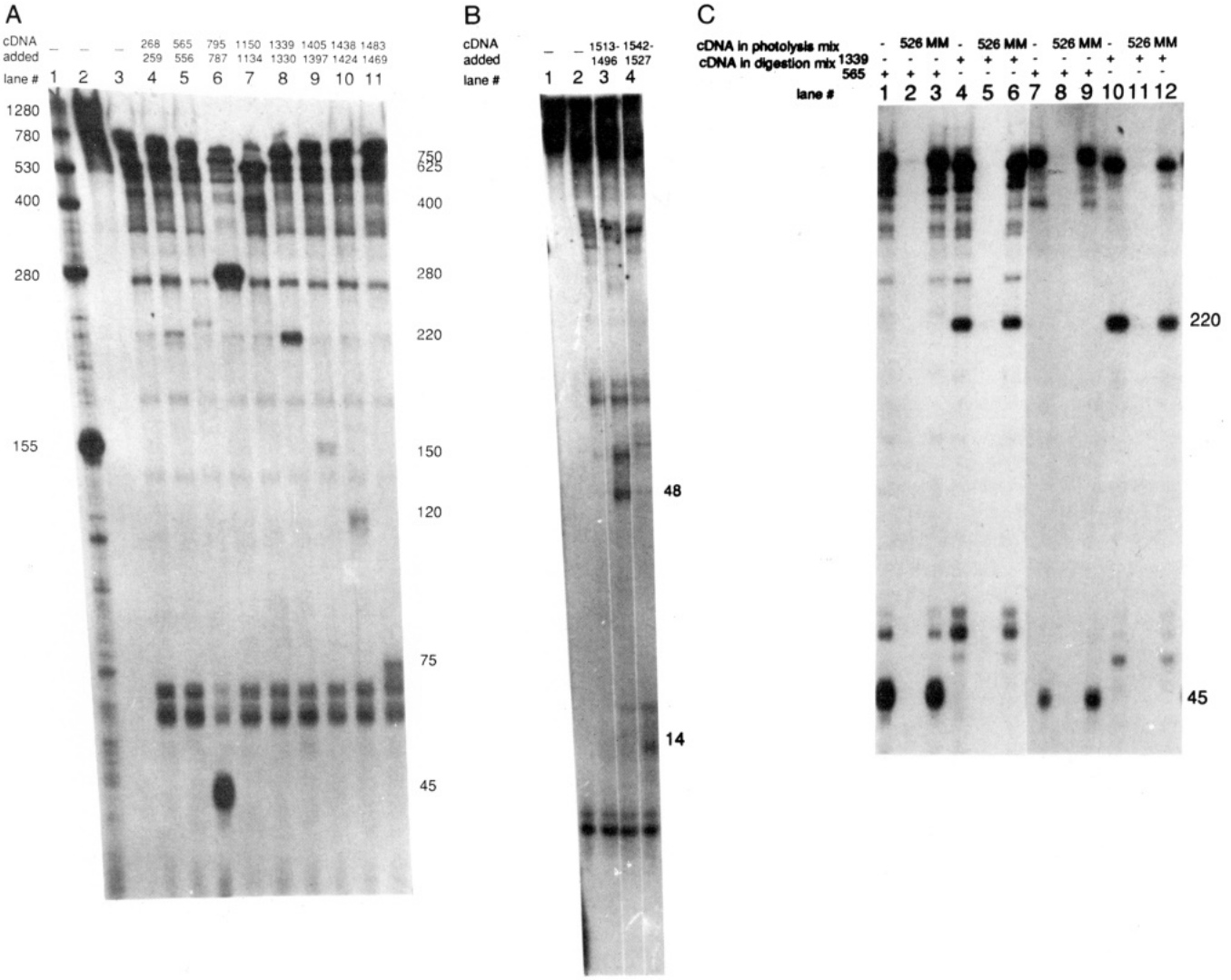

FIGURE 8: Autoradiograms of PAGE analyses of 16S rRNA photolabeled with ABAH526–518A* and digested with RNase H. In a typical experiment, labeled rRNA (5 pmol) prepared from activated subunits and purified by sucrose gradient centrifugation (Figure 7) was incubated with 10 pmol of the indicated cDNA probe in 10 μL of TND buffer and digested with RNase H. Panel A: 5% polyacrylamide gel. Lane 1, DNA size markers; lane 2, labeled 16S rRNA in the absence of RNase H. Samples for lanes 3–11 were digested with RNase H. Lane 3, no added cDNA; lane 4, cDNA 268–259; lane 5, cDNA 565–556; lane 6, cDNA 795–787; lane 7, cDNA 1150–1134; lane 8, cDNA 1339–1330; lane 9, cDNA 1405–1397; lane 10, cDNA 1438–1424; lane 11, cDNA 1483–1469. The labeled fragments in the range 60–75 nt arise from RNaseH-dependent cleavages in the region of 16S rRNA around 576–586 that are independent of added cDNA. Panel B: 12% polyacrylamide gel. Lane 1, labeled 16S rRNA in the absence of RNase H. Samples for lanes 2–4 were digested with RNase H. Lane 2, no added cDNA; lane 3, cDNA 1513–1496; lane 4, cDNA 1542–1527. Fragment sizes estimated from RNA standards are indicated at right. Panel C: 5% polyacrylamide gel. Lanes 1–6: 16S rRNA prepared from activated subunits labeled by ABAH526–518A*. Labeling experiments were carried out in the absence of added cDNA (lanes 1 and 4), in the presence of cDNA 526–518 (lanes 2 and 5), and in the presence of MM-cDNA 526–518 (lanes 3 and 6). RNase H digestions were carried out in the presence of either cDNA 565–556 (lanes 1–3) or cDNA 1339–1330 (lanes 4–6). Lanes 7–12 repeat lanes 1–6, except that 16S rRNA was extracted from labeled SI subunits. The fragment at 55 nt present in lanes 4–6 and 10–12 is due to cleavage in the region 1490–1499, which cDNA 1339–1330 matches at 9 of 10 nucleotides.

4 and 5) and is hardly affected when MM-cDNA 526–518 is present in the photolysis mix (compare lanes 1 and 3 and lanes 4 and 6). The same two labeled fragments are site-specifically labeled in SI subunits (Figure 8C, lanes 7–12), but as compared with activated 30S subunits, labeling of the 45-nt fragment is strongly reduced, while labeling of the 220-nt fragment proceeds to approximately the same extent. Similar analysis shows that labeling of both fragments is strongly reduced in LI subunits.

*Identification of 16S rRNA Nucleotides Labeled by ABAH526–518A**. The specific nucleotides labeled by ABAH526–518A* within the 518–526 to 556–565 region of activated 30S subunits were identified by primer extension (Muralikrishna & Cooperman, 1991). Both ABAH526–518-photolabeled 16S rRNA and control 16S rRNA, prepared from 30S subunits photolyzed in the absence of probe, were hybridized to single-stranded oligodeoxynucleotide primers complementary to 16S rRNA, and the resulting heteroduplexes were examined as substrates for AMV-RT by PAGE and autoradiographic analysis. Using the cDNA primer 590–573, stops or pauses dependent on the presence of covalently bound ABAH526–518 are found at C526, G527, and C528 (Figure 9), giving evidence for photoincorporation into nucleotides C525, C526, and G527. As expected from the results in Figure 8, no photoincorporation-dependent stop sites are observed in the region (nucleotides 570–777) investigated with the cDNA primer 796–781 (data not shown). The primer extension approach is not useful for locating the ABAH526–518A* labeling site falling between nucleotides 1539 and 1542 with greater precision.

Effect of OligoDNA Probes on Chemical Footprinting. The effects of added cDNA 526–518, ABAH526–518, or MM-cDNA 526–518 on the reactivity toward dimethyl sulfate of adenines (at the N1 position) and cytosines (at the N3 position) in the 16S rRNA region 400–570 of activated 30S subunits are presented in Figure 10. In this experiment cDNA 590–

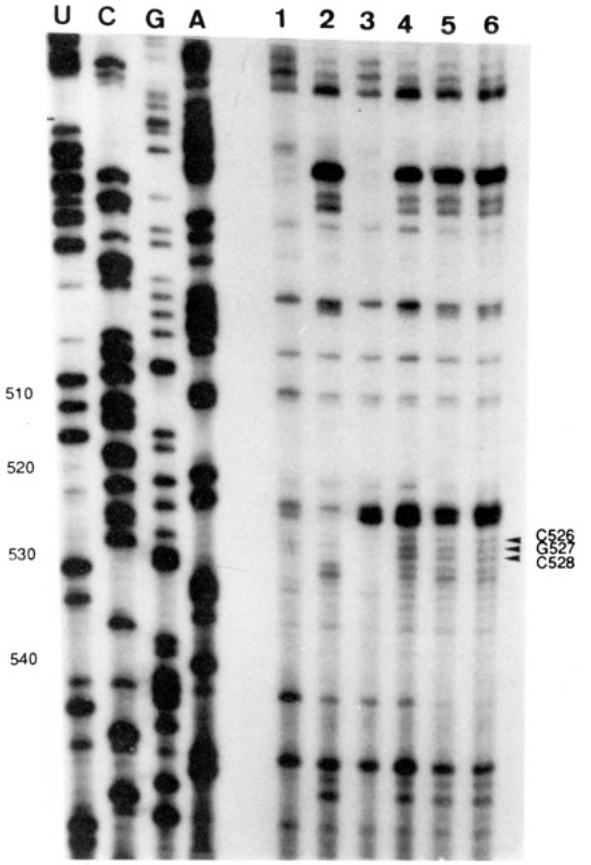

FIGURE 9: Autoradiogram of primer extension with the primer cDNA 590–573 on 16S rRNA labeled with ABAH526–518. Photoincorporation was performed using 150 pmol of activated 30S subunits in a reaction volume of 75 μL: lane 1, no photolysis; lane 2, photolyzed, no ABAH526–518 probe; lane 3, no photolysis, with 3 nmol of probe; lane 4, photolyzed, 0.75 nmol of probe; lane 5, photolyzed, 1.5 nmol of probe; lane 6, photolyzed, 3 nmol of probe. Lanes U, C, G, and A are sequencing products generated in the presence of ddATP, ddGTP, ddCTP, and ddTTP, respectively. Nucleotides at which pauses or stops induced by photoincorporation of ABAH526–518 are observed are indicated.

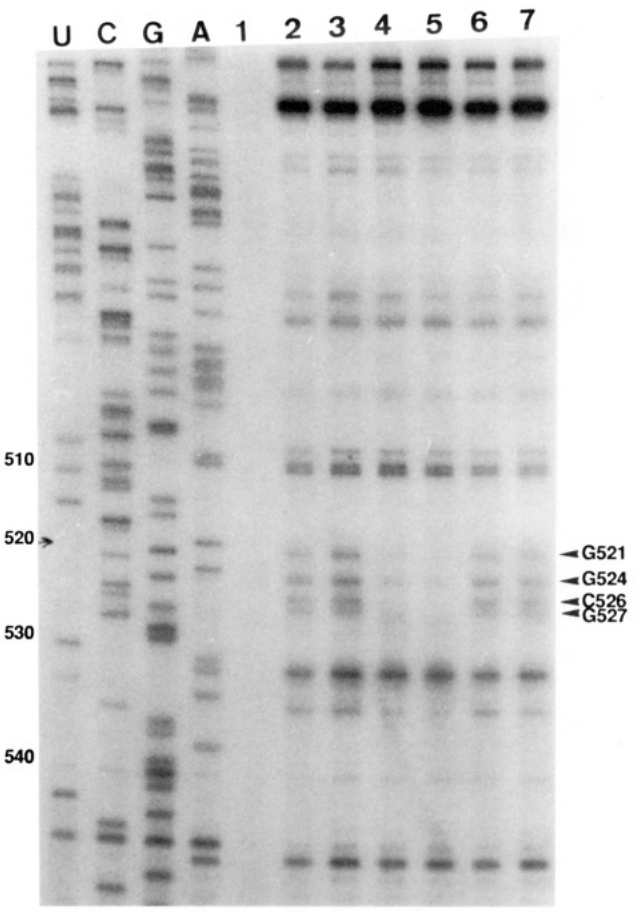

FIGURE 10: Autoradiogram of primer extensions with the primer cDNA 590–573 on 16S rRNA extracted from activated 30S subunits reacted with dimethyl sulfate in the absence and presence of excess added oligoDNA. Lane 1, no added DMS, no added oligoDNA; lane 2, 1 μL of DMS, no added oligoDNA; lane 3, 2 μL of DMS, no added oligoDNA; lanes 4–7, 1 μL of DMS. Lane 4, +cDNA 526–518; lane 5, +ABAH526–518; lane 6, +MM-cDNA 526–518; lane 7, +cDNA (23S rRNA) 811–803. Lanes U, C, G, and A are sequencing products generated in the presence of ddATP, ddGTP, ddCTP, and ddTTP, respectively. Nucleotides protected from methylation in lanes 4 and 5 are indicated.

573 serves as a primer for reverse transcription elongation. Protection of the nucleotides A520, A523, C525, and C526 is observed in the presence of either cDNA 526–518 or ABAH526–518, as expected. In contrast, MM-cDNA 526–518 offers no such protection, nor does the unrelated 23S rRNA-directed cDNA 811–03. No other alterations in reactivity toward dimethyl sulfate are observed in this region. Similarly, no alteration in reactivity is observed in the region 1270–1443, primed by cDNA 1461–1445 (data not shown).

DISCUSSION

In this paper we utilize photoincoporation of a photolabile deoxyoligonucleotide probe to investigate 30S subunit internal structure surrounding the 530 loop. As determined by van Waes et al. (1993), this loop is available toward binding by deoxyoligonucleotide probes only in isolated 30S subunits, as in the current study, or in static 70S ribosomes (tight couples). The reactivities of C525 and C526 toward dimethyl sulfate (Figure 10) are also consistent with a single-stranded 530 loop. On the other hand, Watson–Crick base pairing between bases 524–526 and 505–507, leading to pseudoknot formation, appears to be crucial for ribosomal function, as suggested by Woese and Gutell (1989) and verified by site-specific mutational studies by Powers and Noller (1991). It would appear that the 530 loop exists in at least two conformations within the 30S subunit, one with the pseudoknot and one without. The presence of tRNA, factors, or mRNA prevents deoxyoligonucleotide probe binding (van Waes et al., 1993), suggesting that distribution between these forms may vary as a function of the state of the 30S subunit. Other than at the target site, added cDNA 526–518 or ABAH526–518 has no effect on base reactivity of 16S rRNA regions 400–571 and 1270–1443, from which we infer that oligoDNA binding does not change the distribution between the different conformations of the 530 loop; i.e., they are not in mobile equilibrium.

Our results provide compelling evidence that portions of proteins S3, S4, S7, and S12 as well as the 3′-terminus of 16S rRNA all fall within 24 Å of C526, as 24 Å is the maximum distance between C526 and the nitrene photogenerated from ABAH526–518A*. These results confirm that proteins S4 and S12 are near the 530 loop and provide support for the proximity of the 530 loop to the decoding region of the 30S subunit (Dontsova et al., 1992, Powers & Noller, 1993). They also lead to the suggestion that accounting for all of the results concerning 30S subunit internal structure may require explicit consideration of a multistate model of subunit conformation.

Confidence in the validity of these general conclusions depends upon the clear demonstration that the sites of photoincorporation identified as specific do arise from photolyzed ABAH526–518A* bound to its target site. This specificity is demonstrated by three results obtained in experiments on both activated and inactivated 30S subunits. First, RNase H cleavage of the heteroduplex formed between

ABAH526–518 and 16S rRNA within 30S subunits produces the appropriate 520-nt fragment, as presented in Figure 2. Second, as identified by reverse transcriptase analysis, C525, C526, and G527, nucleotides within or adjacent to the target site, constitute the major site of ABAH526–518A* photoincorporation into 16S rRNA from activated 30S subunits and are also labeled in inactivated 30S subunits (Figures 8 and 9). Third, photoincorporation into proteins S3, S4, S7, and S12 and the two regions of labeled 16S rRNA is reduced when photolysis is carried out in the presence of the competing nonphotolabile probe cDNA 526–518; the presence of the mismatched MM-cDNA 526–518, designed not to bind the target site, does not affect photoincorporation (Figures 3 and 8C). In an experiment performed only on activated 30S subunits, cDNA 526–518 and ABAH526–518 protect nucleotides A520, A523, C525, and C526 from modification by dimethyl sulfate, while MM-cDNA 526–518 does not (Figure 10), also demonstrating the site-specific nature of ABAH526–518 binding.

Photoincorporation of ABAH526–518A* into proteins S3, S4, and S12 is fully in accord with results from prior studies of the 530 loop. Nucleotides in the 530 stem and loop are protected from chemical modification by S4 and S12 (Stern et al., 1989), and mutations in the loop mimic mutations in S12, which affect streptomycin resistance, and in S4, which affect stop codon readthrough and frameshifting frequency (O'Connor et al., 1992). Furthermore, mRNA photoaffinity labeling studies of Brimacombe and co-workers (Rinke-Appel et al., 1991; Dontsova et al., 1992) have shown that a photolabile group at the +11 position of bound mRNA (where positions +1 through +3 correspond to the AUG initiation codon) incorporates into both A532 and protein S3. Additional evidence that S3, S4, S12, and the 530 loop form a neighborhood within the 30S subunit comes from experiments demonstrating that the pairs of proteins S3–S4, S3–S12, and S4–S12 can be cross-linked to one another [summarized in Lambert et al. (1983)] and that all three proteins can be photoincorporated within the 504–615 region of 16S rRNA substituted with 4-thiouridine (Hajnsdorf et al., 1989).

Photoincorporation of ABAH526–518A* into the 3′-terminus of 16S rRNA and protein S7 from the same target site is consistent with the results of Greuer et al. (1987) identifying a direct cross-link between S7 and the 3′-terminus. Also in mRNA photoaffinity labeling studies by Brimacombe and co-workers (Stade et al., 1989; Dontsova et al., 1991), photolabile groups at positions –2, –3, –5, and –8 of bound mRNA photoincorporate into S7, and groups at –2, –4, and –8 photoincorporate into the 3′-terminus of 16S rRNA.

Our results clearly address the current controversy concerning the physical proximity of the 530 loop to both the 3′-end of tRNA and the 1400 decoding region. The rRNA photo-cross-linking results show that C526 lies within 24 Å of the 3′-terminal region. Moreover, both ABAH526–518A* and ABAH1405–1397A* photoincorporate specifically into S7, yielding identical labeled tryptic fragments (Figure 6); these rRNA regions must therefore be within 48 Å of each other, and perhaps considerably closer. Our results are fully in accord with the demonstration by Dontsova et al. (1992) that a 14-nt region of mRNA yields cross-links to the 3′-terminus of 16S rRNA, to nucleotides in the 1400 region, and to A532. Together, these results support Trifonov's (1987, 1992) proposal, based on sequence complementarity to frequently occurring codons, that the regions 517–534, 1392–1408, and 1530–1542 are likely mRNA binding zones in 16S rRNA. On the other hand, our results appear to be inconsistent with direct protein–protein distance measurements, as determined by the neutron diffraction studies of Moore and co-workers (Capel et al., 1988). They measure centers-of-mass distances of 112 Å for S7–S12 and 114 Å for S7–S4. Yet we conclude, on the basis of the near identity in K_d values for inhibition of labeling with added cDNA 526–518 (Figure 5) in activated 30S subunits, that S3, S4, S7, and S12 are all labeled by ABAH526–518A* from a common site, so that portions of these proteins must lie within 48 Å of one another. A similar inconsistency between the mRNA cross-linking results and the neutron diffraction 30S protein map led Powers and Noller (1993), in a study of the effects of a G530A mutation, to discount Brimacombe's conclusion that the 530 loop is physically close to the decoding site. Rather, Powers and Noller maintain that effects of the 530 mutation on A-site function, as well as the earlier result that A-site-bound tRNA protects nucleotides in the 1400 and 1500 regions and in the 530 loop (Moazed & Noller, 1986), are likely to arise from allosteric rather than direct interaction. The recent results of Santer et al. (1993) showing that a G530U mutation produces ribosomes phenotypically similar to those with base-pairing disruptions in the decoding region could be accounted for in like manner.

Several explanations might be offered to account for the apparent inconsistency cited above, including simple error in either the execution or the interpretation of the experiments under consideration or severe eccentricity in the shapes of proteins S4, S7, and/or S12 within the 30S subunit, such that portions of S7 could come within 48 Å of either S4 or S12, despite the large distances between their centers of mass. At present there is no evidence for the validity of either possibility, and we would like to consider a third, that these inconsistencies may reflect experiments performed employing ribosomal subunits having differing conformations. Such structural variations could be particularly apparent in the decoding center, which may fall in a highly flexible portion of the 30S subunit. In fact, Moazed et al. (1986b) have shown that changes in nucleotide chemical reactivity following the 30S inactivated to activated transition are concentrated in the 1400, 1500, and 3′-terminal regions of 16S rRNA. Our results show dramatic differences in labeling patterns for both ABAH526–518A* and ABAH1397–1405A* (Muralikrishna & Cooperman, 1994) following this transition and therefore also support the notion of structural flexibility predicted by a multistate model. Furthermore, the 1400 region (Muralikrishna & Cooperman, 1994) and the 530 loop each exist in at least two conformations: one which is single-stranded and open to heteroduplex formation with probe cDNAs and one which has internal base pairing.

The experiments of Brimacombe and co-workers using photolabile mRNA probes were performed using activated 30S subunits or 70S ribosomes, whereas those of Capel and co-workers (Capel et al., 1988) were performed on reconstituted 30S subunits in a buffer containing 0.5 mM Mg^{2+}, a condition that affords inactivated 30S subunits (Zamir et al., 1974). It is tempting to use this difference to rationalize the observed contradictions in terms of a two-state model. Thus the proximity of S7 and the 3′-end of 16S rRNA to the 530 loop observed both by Brimacombe and co-workers and by us could be attributed to the activated conformation, while the large S4-S7 and S12-S7 distances of Moore's model (Capel et al., 1988) could arise from the inactivated conformation. Our finding that ABAH526–518A* photoincorporation into the 3′-end of 16S rRNA and S7 is preserved or enhanced in SI subunits demonstrates the inadequacy of this simple two-state model. Rather, we must consider the possibility that the 30S subunit has multiple conformational states, and that the

topographical relationships between particular ribosomal components may differ widely between different states. Bhangu and co-workers (Bhangu et al., 1994) have reached a similar conclusion in recent work tracing the pathway of mRNA on the ribosome. Efforts to model the internal structure of 30S subunits (Brimacombe 1988, 1992; Stern et al., 1988; Malhotra et al., 1990; Malhotra & Harvey, 1994), using data obtained from several laboratories utilizing different 30S preparations, may therefore require explicit consideration of a multistate model of subunit conformation.

The functionally important conformational changes accompanying the transition from activated to inactivated 30S subunits (Zamir et al., 1974) are accompanied in the present work by the changes in labeling observed on photoincorporation of ABAH526–518A* into ActA, ActB, SI, and LI subunits. Interestingly, labeling of the 3′-end of 16S rRNA and of its associated protein S7, involving a bridging between the two regions of rRNA, is either enhanced (S7) or preserved (3′-end) in SI subunits (Table 1; Figure 8C), whereas labeling of the nucleotides within the 530 loop itself, as well as of the proteins (S3/S4 and S12) directly associated with the 530 loop, is diminished. Recently, photolabeling of SI and activated 30S subunits by ABAH1397–1405A* was also shown to display differences. In this case S3/S4 was more highly labeled in the SI subunit, while labeling of S7 was higher in the activated subunit (Muralikrishna & Cooperman, 1994). A simple explanation for these results would place these proteins somewhere between the 530 and 1400 regions of 16S rRNA, such that a conformational change which resulted in a protein being more accessible to labeling from one region would make it less accessible to labeling from the other.

ACKNOWLEDGMENT

We acknowledge with thanks the assistance of Dr. Richard Brimacombe in the immunological identification of labeled proteins and the excellent technical assistance of Ms. Nora Zuño.

REFERENCES

Bhangu, R., Juzumiene, D., & Wollenzein, P. (1994) *Biochemistry 33,* 3063–3070.

Brimacombe, R. (1988) *Biochemistry 27*, 4207–4214.

Brimacombe, R. (1992) *Biochimie 74*, 319–326.

Buck, M. A., Olah, T. V., Weitzmann, C. J., & Cooperman, B. S. (1989) *Anal. Biochem. 182*, 295–299.

Capel, M. S., Kjeldgaard, M., Engelman, D. M., & Moore, P. B. (1988) *J. Mol. Biol. 200*, 65–87.

Cooperman, B. S. (1980) in *Ribosomes: Structure, Function, & Genetics* (Chambliss, G., Craven, G. R., Davies, J., Davis, K., Kahan, L., & Nomura, M., Eds.) pp 531–554, University Park Press, Baltimore.

Cooperman, B. S., Muralikrishna, P., & Alexander, R. W. (1993) in *The Translational Apparatus* (Nierhaus, K. H., Subramanian, A. R., Erdmann, V. A., Franceschi, F., & Wittman-Liebold, B., Eds.) pp 465–476, Plenum Press, New York.

Dontsova, O., Kopylov, A., & Brimacombe, R. (1991) *EMBO J. 10*, 2613–2620.

Dontsova, O., Dokudovskaya, S., Kopylov, A., Bogdanov, A., Rinke-Appel, J., Jünke, N., & Brimacombe, R. (1992) *EMBO J. 11*, 3105–3116.

Giri, L., Hill, W. E., Wittmann, H. G., & Wittmann-Liebold, B. (1984) *Adv. Protein Chem. 36*, 1–78.

Girshovich, A. S., Bochkareva, E. S., Kramarova, V. A., & Ovchinnikova, Y. A. (1974) *FEBS Lett. 42*, 213–217.

Greuer, B., Osswald, M., Brimacombe, R., & Stöffler, G. (1987) *Nucleic Acids Res. 15*, 3241–3255.

Gutell, R. R., Weiser, B., Woese, C. G., & Noller, H. F. (1985) *Prog. Nucleic Acid Res. Mol. Biol. 32*, 155–216.

Hajnsdorf, E., Favre, A., & Expert-Bezançon, A. (1989) *Nucleic Acids Res. 17*, 1475–1491.

Hill, W. E., Weller, J., Gluick, T., Merryman, C., Marconi, R. T., Tassanakajohn, A., & Tapprich, W. E. (1990) in *The Ribosome: Structure, Function, & Evolution* (Hill, W. E., Dahlberg, A., Garrett, R. A., Moore, P. B., Schlesinger, D., & Warner, J. R., Eds.) pp 93–106, American Society for Microbiology, Washington, DC.

Kerlavage, A. R., Hasan, T., & Cooperman, B. S. (1983) *J. Biol. Chem. 258*, 6313–6318.

Lambert, J. H., Boileau, G., Cover, J. A., & Traut, R. R. (1983) *Biochemistry 22*, 3913–3920.

Langer, J. A., & Lake, J. A. (1986) *J. Mol. Biol. 187*, 617–621.

Lasater, L. S., Montesano-Roditis, L., Cann, P. A., & Glitz, D. G. (1990) *Nucleic Acids Res. 18*, 477–485.

Malhotra, A., & Harvey, S. C. (1994) *J. Mol. Biol. 240*, 308–340.

Malhotra, A., Tan, R. K.-Z., & Harvey, S. C. (1990) *Proc. Natl. Acad. Sci. U.S.A. 87*, 1950–1954.

Melançon, P., Lemieux, C., & Brakier-Gingras, L. (1988) *Nucleic Acids Res. 16*, 9631–9639.

Moazed, D., & Noller, H. F. (1986) *Cell 47*, 985–994.

Moazed, D., & Noller, H. F. (1987) *Nature 327*, 389–394.

Moazed, D., Stern, S., & Noller, H. F. (1986a) *J. Mol. Biol. 187*, 399–416.

Moazed, D., Van Stolk, B. J., Douthwaite, S., & Noller, H. F. (1986b) *J. Mol. Biol. 191*, 483–493.

Muralikrishna, P., & Cooperman, B. S. (1991) *Biochemistry 30*, 5421–5428.

Muralikrishna, P., & Cooperman, B. S. (1994) *Biochemistry 33*, 1392–1398.

Oakes, M. I., & Lake, J. A. (1990) *J. Mol. Biol. 211*, 897–906.

Oakes, M. I., Kahan, L., & Lake, J. A. (1990) *J. Mol. Biol. 211*, 907–918.

O'Connor, M., Göringer, H. U., & Dahlberg, A. E. (1992) *Nucl. Acids Res. 20*, 4221–4227.

Powers, T., & Noller, H. F. (1990) *Proc. Natl. Acad. Sci. U.S.A. 87*, 1042–1046.

Powers, T., & Noller, H. F. (1991) *EMBO J. 10*, 2203–2214.

Powers, T., & Noller, H. F. (1993) *Proc. Natl. Acad. Sci. U.S.A. 90*, 1364–1368.

Rinke-Appel, J., Jünke, N., Stade, K., & Brimacombe, R. (1991) *EMBO J. 10*, 2195–2202.

Santer, M., Santer, U., Nurse, K., Bakin, A., Cunningham, P., Zain, M., O'Connell, D., & Ofengand, J. (1993) *Biochemistry 32*, 5539–5547.

Shen, Z., & Fox, T. D. (1989) *Nucleic Acids Res. 17*, 4535–4539.

Stade, K., Rinke-Appel, J., & Brimacombe, R. (1989) *Nucleic Acids Res. 17*, 9889–9908.

Stern, S., Weiser, B., & Noller, H. F. (1988) *J. Mol. Biol. 204*, 447–481.

Stern, S., Powers, T., Changchien, L., & Noller, H. F. (1989) *Science 244*, 783–790.

Trifonov, E. N. (1987) *J. Mol. Biol. 194*, 643–652.

Trifonov, E. N. (1992) *Biochimie 74*, 357–362.

van Waes, M. A., Smith, C. E., & Hill, W. E. (1993) *FASEB J. 7*, A1093 (Abstract 236).

Woese, C. R., & Gutell, R. R. (1989) *Proc. Natl. Acad. Sci. U.S.A. 86*, 3119–3122.

Woese, C. R., Fox, G. E., Zablen, L., Uchida, T., Bonen, K., Pechman, K., Lewis, B. J., & Stahl, D. (1975) *Nature 254*, 83–86.

Zamir, A., Miskin, R., & Elson, D. (1971) *J. Mol. Biol. 60*, 347–364.

Zamir, A., Miskin, R., Vogel, Z., & Elson, D. (1974) *Methods Enzymol. 30*, 406–426.